Surface effects and ferroelectric phase transitions in $BaTiO_3$ ultrathin films

S. Tinte and M. G. Stachiotti
Instituto de Física Rosario, Universidad Nacional de Rosario, 27 de Febrero 210 Bis, 2000 Rosario, Argentina
(Received 9 July 2001; published 8 November 2001)

We present a finite-temperature study of ferroelectric phase transitions in $BaTiO_3$ ultrathin films using an atomic-level simulation approach. This is based on a shell model for $BaTiO_3$ with parameters obtained from first-principles calculations. While transitions involving in-plane electric polarization are practically unperturbed by the presence of the surface, surface atomic relaxations act as a strong perturbation on the ferroelectric order perpendicular to the surface. However, a strain induced ferroelectric polydomain phase with an out-of-plane orientation of polarization is stabilized in a not short-circuited film as thin as 20 Å. A reduction of the out-of-plane polarization at the film surface is observed.

DOI: 10.1103/PhysRevB.64.235403 PACS number(s): 77.55.+f, 77.80.Dj, 77.84.Dy

I. INTRODUCTION

The potential utilization of ferroelectric (FE) thin films in a new generation of devices has driven a large amount of research worldwide. These have as a general advantage reduced size and weight, which can be exploited, for example, in the fabrication of high-density nonvolatile random access memories.[1] For that reason, the question of the minimum film thickness with switching polarizations is a crucial point. Recently, high quality films of $PbZr_{0.2}Ti_{0.8}O_3$ grown on Nb-doped (001) $SrTiO_3$ single-crystal substrates have been observed to exhibit ferroelectricity down to a thickness of 4 nm.[2] However, what is the thinnest ferroelectric layer that can still yield stable polarization remains as an unsolved question.

Phenomenological theories have provided a deep insight into the FE properties of thin films. Wang *et al.*[3] calculated the spontaneous polarization and electrostatic potential in FE films with domain structure. They found that the polarization is reduced at the film surface; and, from a free-energy analysis, they led to the conclusion that ferroelectricity of very thin films with domain structure may be unstable. An abrupt transition from a monodomain to a polydomain state has been found in FE thin films with a passive (nonferroelectric) layer at the FE-electrode interface.[4] It was shown that this domain structure, which is important for the problem of switching, exists for any value of the passive layer thickness. Regarding the effect of the film-substrate misfit strain, a phenomenological thermodynamic theory of FE thin films epitaxially grown onto cubic substrates predicts distinct phases depending on the misfit strain.[5] It was also shown that the 2D clamping and straining of the film by the substrate leads to the appearance of ferroelectricity in $SrTiO_3$ films.[6]

These are just a few representative examples of the important role played by the phenomenological theories in the understanding of FE thin film properties. However, these type of theories are based on the continuous medium approximation and, therefore, they are not applicable for ultrathin films where an accurate atomic-level description is necessary. The indispensability of an atomic-level approach was borne out by recent first-principles calculations on $BaTiO_3$ slabs,[7,8] which demostrated that the surface relaxation energies are many times larger than the bulk ferroelectric well depth, which would indicate that the surface is capable of acting as a strong perturbation on the ferroelectric order. Recently, an effective Hamiltonian approach[9] showed that, under short-circuit electrical boundary conditions, $PbTiO_3$ films as thin as three unit cells exhibit a perpendicularly polarized ground state, with significant enhancement of the polarization at the surface. However, this model does not include surface relaxation effects.

Although first-principles methods are extremely precise, they are quite computer demanding. So, these calculations are restricted to the investigation of zero-temperature properties of perovskites involving a rather small number of atoms. For the study of the thermal behavior, or to handle larger system sizes, other methods are necessary. Recently, we have developed an atomistic model for $BaTiO_3$ (Ref. 10) by mapping first-principles underlying potential surfaces. In the present paper we address the question of how the ferroelectric phase transitions of bulk $BaTiO_3$ are modified in ultrathin films using the same atomistic model. The phase transition sequence in a not short-circuited stress-free ultrathin film is studied by molecular dynamics simulations. As an important factor which can influence ferroelectricity is the strain effect produced by the lattice mismatch between a given substrate and the ultrathin film, we investigate the effects produced by the strain on the ferroelectric properties of the ultrathin film.

II. MODEL AND COMPUTATIONAL DETAILS

The atomistic model for bulk $BaTiO_3$ was developed by mapping first-principles potential energy surfaces for various configurations of some carefully selected atomic displacements. The potential parameters were obtained by performing a fit of interatomic potentials to these energy surfaces. The first-principles total energy calculations were done within the local density approximation to density functional theory, using the full-potential LAPW method.

For the atomistic simulation we chose the nonlinear oxygen polarizability model. Here each ion is modeled as a massive core linked to a massless shell. An anisotropic core-shell interaction is considered at the O^{-2} ions, with a fourth-order core-shell interaction along the O-Ti bond. This emphasizes the large anisotropic polarization effects at the oxygens pro-

duced by variations of the Ti-O distance. In addition to the Coulombic interactions, the model contains pairwise short-range potentials which are defined as $V(r)=ae^{(-r/\rho)}-c/r^6$. These potentials account for the effects of the exchange repulsion together with the van der Waals attraction between atoms. The material-specific potential parameters were determined by fitting the model energy behavior to first-principles results. See Ref. 10 for more details of the model building.

The resulting model was able to reproduce delicate properties of $BaTiO_3$ in very good agreement with first-principles and experimental data. The model yields clear ferroelectric instabilities with similar energetics compared with the LAPW calculations. Energy lowerings of $\approx$1.2, 1.65, and 1.9 mRy/cell are obtained for the (001), (011), and (111) ferroelectric mode displacements, respectively. The model also reproduces several zero-temperature properties which are relevant for this material: bulk modulus, Born effective charges, the presence of two-dimensional instabilities in the phonon dispersion curves, Γ-phonon frequencies, and eigenvectors.[10]

The temperature-dependent properties of the bulk material were investigated by constant-pressure molecular dynamics (MD) simulations. We showed that the nontrivial phase transition sequence (cubic-tetragonal-orthorhombic-rombohedral) was correctly reproduced. An excellent overall agreement with the experimental data was obtained for the structural parameters and expansion coefficients, showing that the model reproduces the delicate structural changes involved in the transitions. The drawback is, however, that the theoretically determined transition temperatures (190, 120, and 90 K) tend to be too small compared with experiment (393, 278, 183 K). A similar behavior was obtained by an effective Hamiltonian approach whose parameters were also fitted to first-principles calculations.[11]

The model also provides a good description of the nature of the dynamics in each phase, where order-disorder was found to be the dominant dynamical mechanism for the transitions.[12] This mechanism leads to the presence of a rhombohedral local enviroment of Ti in all phases. This local structure appears because of the slow dynamics associated with a relaxational motion of local polarizations, which correlate within chainlike precursor domains in the paraelectric phase.

In the present paper we consider a (001) TiO_2-terminated slab of 28 Å width to perform molecular dynamics (MD) simulations. The study is carried out using the DL-POLY package,[13] where the adiabatic dynamics of the electronic shells is approximated by assigning small masses to them. The runs were performed employing a Hoover constant-$(\bar{\sigma},T)$ algorithm; all cell lengths and cell angles were allowed to fluctuate. Our calculations are carried out in a periodic slab geometry, as it is usual in first-principles calculations of surface properties. The slab is 28 Å thick containing 8 TiO_2 layers and 7 BaO layers ($6\times6\times7.5$ unit cells, 1368 atoms). To minimize the interaction between periodic images, a vacuum region of 20 Å separates the periodic slabs. We tested the sensibility of the results with respect to the vacuum region size: by increasing the vacuum gap by 20%, the resulting polarization profiles changed by less than 0.5%. The reason for this almost negligible interaction between periodic images comes out from the fact that, in all the cases analyzed in this paper, the net out-of-plane polarization of the slab is zero. So, there is no a dipole-dipole interaction between images but only higher order multipole-multipole interactions, which are weaker. In this sence, the slab could be consider as isolated.

III. RESULTS AND DISCUSSIONS

A. Static surface effects

The achievements reached by our model in the description of the bulk properties do not necessarily indicate that the same model (i.e. with the same parameters) is able to reproduce $BaTiO_3$ surface effects. As our final goal is to perform finite-temperature simulations on ultrathin films, it is very important to check if the bulk model describes properly the static surface properties of $BaTiO_3$. Although a comparison with experimental data is, of course, the best way to validate a model, experimental studies of perovskites surfaces are complicated by the difficulties of preparing clean and defect-free surfaces. Therefore, most experimental investigations have not been very conclusive. Furthermore, we are not aware of experimental studies of $BaTiO_3$ surfaces. So, we take recent first-principles total-energy calculations on periodic slabs[7,8] as benchmark results to compare with. To this end, we determined the equilibrium atomic positions for the same kind of slabs used in the *ab initio* calculations. Although the detailed results of this comparison with *ab initio* results have been recently published,[14] we would like to highlight several achievements. So, in this section we present static calculations on periodic slabs of $BaTiO_3$ to compare atomic relaxations and surface energies with the above mentioned *ab initio* studies of $BaTiO_3$ surfaces. This constitutes a very important initial step in order to validate the model to perform a further finite-temperature study.

Padilla and Vanderbilt[8] studied symmetrically BaO terminated and TiO_2 terminated slabs of tetragonal and cubic $BaTiO_3$ whose coordinates have been fully relaxed by minimizing the total energy. Therefore, a comparison with their results could be considered as a very exigent test for our model. Following their steps, we first determined the equilibrium atomic positions for the two types of slabs in the cubic phase, starting from the ideal structure. By symmetry, there are no forces along the *x* and *y* directions for the cubic surfaces, so we only compare the atomic displacements along the *z* direction, which is perpendicular to the surface. As in the first-principles calculations,[8] each slab contains seven layers of atoms and the vacuum region is three lattice constants thick. The results are listed in Table I, together with the *ab initio* results which are shown in parentheses. It is worth mentioning that the relaxation patterns obtained with the model are in full agreement with the *ab initio* ones. In particular, the model reproduces satisfactorily the relaxation direction of the surface-layer atoms, which move inwards the slab (this is indicated by a negative sign in the table). Regarding the magnitude of the atomic displacements, they are, in general, slightly overestimated with respect to the first-principles results; except for the first-layer atoms of the BaO surface, which are underestimated.

TABLE I. Atomic relaxations of the TiO_2 (left panel) and BaO-terminated (right panel) surfaces in the cubic (*C*) phase, given as percent of theoretical unit cell parameter *a*, with repect to ideal positions. For comparison, *ab initio* results (Ref. 8) are shown in parentheses.

Atom	δ_z (C)	Atom	δ_z (C)
Ti(1)	-4.14 (-3.89)	Ba(1)	-0.72 (-2.79)
$O_I(1)$	-2.74 (-1.63)	$O_{III}(1)$	-1.09 (-1.40)
$O_{II}(1)$	-2.74 (-1.63)	Ti(2)	1.70 (0.92)
Ba(2)	2.36 (1.31)	$O_I(2)$	2.75 (0.48)
$O_{III}(2)$	-0.50 (-0.62)	$O_{II}(2)$	2.75 (0.48)
Ti(3)	-0.81 (-0.75)	Ba(3)	-0.69 (-0.53)
$O_I(3)$	-0.72 (-0.35)	$O_{III}(3)$	-0.28 (-0.26)
$O_{II}(3)$	-0.72 (-0.35)		

As was pointed out by Cohen,[7] the average surface energy can be calculated by adding the energies of the Ba-terminated and the Ti-terminated slabs, which gives the energy of 7 $BaTiO_3$ units. Then, we subtract 7 times the bulk energy per cell and the result corresponds to 4 surfaces. In this way, we obtain the average surface energy for the unrelaxed $[E_{sup}(\text{unrel})]$ and the relaxed $[E_{sup}(\text{relax})]$ cubic slabs. The difference between these energies (ΔE) gives the surface relaxation energy. We compare our calculated values with those obtained previously by *ab initio* calculations in Table II. The agreement is quite good. We note that ΔE is many times larger than the bulk ferroelectric well depth, estimated to be of the order of 0.03 eV.

Finally, in order to study the influence of surface relaxation effects upon the in-plane ferroelectric distortion, we determine the equilibrium atomic positions for the tetragonal phase with FE polarization parallel to the surface in the two symmetric terminated slabs. We compare, in Table III, the average ferroelectric distortion (δ_{FE}) for each layer of the tetragonal slabs, which is defined as $\delta_{FE}=\delta_x(\text{Ba})-\delta_x(O_{III})$ for BaO planes, and $\delta_{FE}=\delta_x(\text{Ti})-[\delta_x(O_I)+\delta_x(O_{II})]/2$ for TiO_2 planes. The bulk values are given for reference in the last row of the table. For the TiO_2-terminated surface, one can see a clear increase in the average ferroelectric distortions δ_{FE} when going from the bulk values to the surface layer. Just the opposite behavior is found for the BaO-terminated surface. So, the principal feature obtained by our calculation (in agreement with the *ab initio* result) is that the in-plane ferroelectricity is strongly enhanced at the Ti-terminated surface and suppressed at the Ba-terminated surface.

TABLE II. Average surface energy for the unrelaxed $E_{sup}(\text{unrel})$ and relaxed cubic slabs $E_{sup}(\text{relax})$, given in eV per surface unit cell. ΔE is the surface relaxation energy.

	$E_{sup}(\text{unrel})$	$E_{sup}(\text{relax})$	ΔE
present calculation	1.359	1.172	0.187
Ref. 8	1.358	1.241	0.117
Ref. 7	0.92		

TABLE III. Average layer-by-layer ferroelectric distortions δ_{FE} of the relaxed slabs, in percent of the theoretical lattice constant *c*. *Ab initio* results (Ref. 8) are shown in parentheses.

	Ti-O terminated		Ba-O terminated	
layer	δ_{FE} (BaO)	δ_{FE} (TiO_2)	δ_{FE} (BaO)	δ_{FE} (TiO_2)
1		4.87 (4.38)	1.07 (1.56)	
2	1.41 (1.44)			1.60 (1.82)
3		3.61 (3.44)	0.81 (1.31)	
4	2.45 (1.65)			2.64 (3.32)
Bulk	2.45 (1.50)	2.32 (3.20)	2.45 (1.50)	2.32 (3.20)

In summary, we have shown that the model developed for the bulk material proves also successful for describing surface properties, such as structural relaxations and surface energies, which are found to be in quite good agreement with recent first-principles total energy calculations. In particular, a very good description is obtained for the TiO_2 surface. For the BaO surface, the description is not so accurate. Nevertheless, the relaxation patterns obtained with the model for both slabs are in full qualitative agreement with the *ab initio* ones. The average surface energy and the relaxation energy are in quite good agreement with first-principles calculations. The energy gain on displacing the surface ions is much greater than the bulk ferroelectric well depth, which indicates that ionic motions on surfaces could indeed dominate the bulk energetics for thin slabs.

B. Phase transition sequence in a stress-free slab

In this section we present the results of molecular dynamics simulations for a (001) TiO_2-terminated stress-free slab of 28 Å width. We chose a TiO_2-terminated slab because, as it was shown in the precedent section, it provides a very precise description of the surface effects when it is compared with *ab initio* results.

In Fig. 1 (top panel) we show the three components of the mean polarization obtained by MD simulations as a function of temperature. P_x and P_y are the polarization components parallel to the slab surface, while P_z is the one perpendicular to the surface. The lattice parameters are displayed in the bottom panel. As it is expected, the polarization component perpendicular to the slab surface is zero at all temperatures, that is the slab cannot develop a net out-of-plane polarization just as a consequence of the boundary conditions used, where the surfaces are not short-circuited. On the other hand, the behavior of the other two components indicates a sequence of transitions which leads to the appearance of ferroelectric phases with in-plane polarization (i.e., polarization parallel to the surface).

In order to clarify the description we have divided the phase diagram, shown in Fig. 1, into four temperature ranges. At high temperatures (stage A), the polarization components are all very close to zero indicating a paraelectric phase. As the system is cooled down (stage B), P_x acquires a value clearly different from zero while $P_y \simeq 0$, and the structure presents a considerable in-plane strain. When the temperature is further reduced to stage C the two mentioned

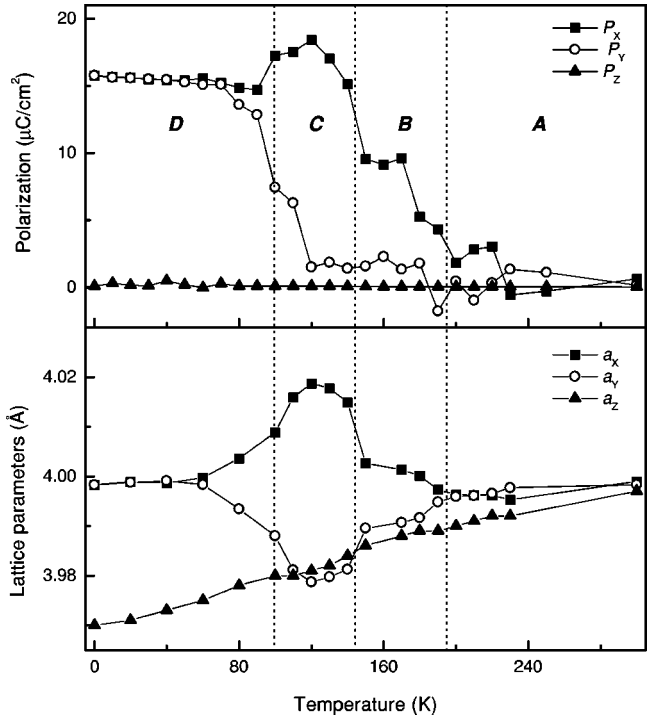

FIG. 1. Phase diagram of the $BaTiO_3$ film resulting from the MD simulations. Top panel: the three components of the average polarization; and bottom panel: the corresponding cell parameters (a_z was calculated as the slab width/7).

features of stage B are magnified. In both stages, B and C, the slab has a net polarization along the (100) direction. Finally, in stage D, $P_x \simeq P_y$ different from zero, and the slab has a net (110) polarization.

The cell-by-cell in-plane polarization profiles across the slab at different temperatures are shown in Fig. 2. All profiles show increments of the local polarization in the two unit cells nearest to the surface, at both sides of the slab. This surface polarization enhancement arises from the fact that we are simulating a TiO_2-terminated slab. On the contrary, we find a decrease of the surface polarization for a BaO-terminated slab. So, the polarization behavior near the surface depends on the surface termination, a fact which is in agreement with the above static results. The local polarizations of the inner cells display a rather flat plateau. The magnitude of the electric polarization for these cells in stages C and D coincides with the bulk polarization components obtained with the model for the tetragonal ($\approx 17 \mu C/cm^2$) and orthorhombic phases ($\approx 14 \mu C/cm^2$), respectively. Moreover, the transition temperatures for the paraelectric-(100) polarized and the (100)-(110) polarized phase transitions practically coincide with the cubic-tetragonal and tetragonal-orthorhombic transition temperatures of the bulk material.[10] These observations lead to the conclusion that ferroelectric phase transitions involving in-plane electric polarization are practically unperturbed by the presence of the surface. One important difference with the bulk is, however, the appearance of a surface phase transition at stage B, where the two unit cells nearest to the surface are polarized, while the inner cells are not [see Fig. 2 (open squares)]. So, in this temperature range, the slab is composed by an in-plane polarized ferroelectric surface layer on both sides of a paraelectric bulk material. Although experimental studies of perovskites surfaces are complicated by the difficulties of preparing defect-free surfaces, the achievement of McKee *et al.*[15] who reported layer-by-layer growth of $BaTiO_3$ on MgO in which the perovskite structure was stabilized at the unit-cell level, should allow a test of the existence of this two dimensional ferroelectric layer.

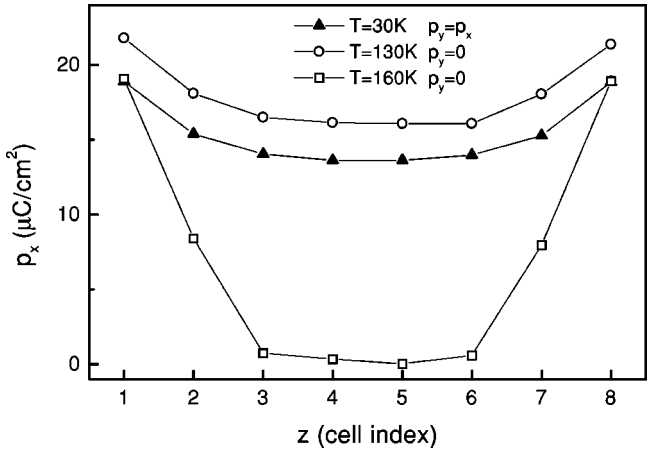

FIG. 2. Cell-by-cell in-plane polarization profiles across the slab at different temperatures.

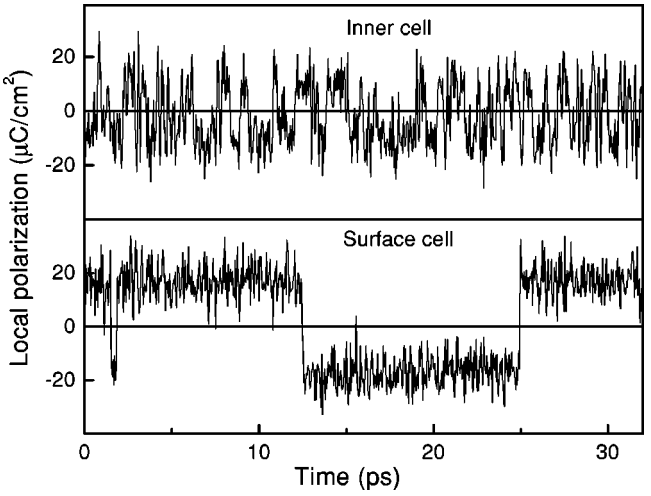

FIG. 3. Time evolution of the local polarization p_x for an inner (top panel) and a surface (bottom panel) cell in the paraelectric phase at $T = 220$ K.

To understand the nature of the microscopic dynamics leading to the presence of this in-plane polarized ferroelectric surface layer, we analyzed, in the high temperature paraelectric phase, the time evolution of local polarizations for a surface and an inner cell. For both we observe in Fig. 3 that fast oscillations around finite polarization values coexist with much slower polarization reversals. Therefore, as in the bulk material,[12] a relaxational slowing-down process is responsible for the appearance of the in-plane polarized phase in the film. Since the relaxation time of the surface cells is ≈ 10 times larger than the one for the inner cells, the polarization

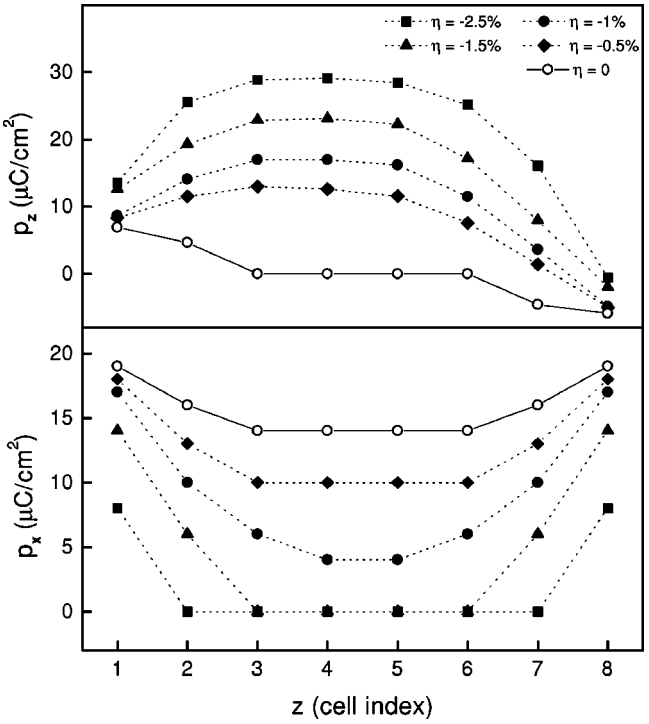

FIG. 4. Cell-by-cell out-of-plane (top panel) and in-plane (bottom panel) polarization profiles of a randomly chosen chain perpendicular to the slab surface for different misfit strains (η) at $T=0$ K. In the in-plane polarization profiles $p_y=p_x$.

''freezes'' first in the surface, in such a way that the surface orders at a higher temperature than the interior of the film.

As was previously shown in Fig. 1, the mean polarization perpendicular to the slab surface is zero at all temperatures. This was expected because the slab cannot develop a net out-of-plane polarization as a consequence of the boundary conditions used. However, a vanishing total polarization could arise from the crystal break into domains. We show that this is not the case by analyzing the polarization profile across the slab, which is presented in the top panel of Fig. 4 [see the case $\eta=0$ (open circles)]. In this figure, the cell-by-cell out-of-plane polarization profile of a randomly chosen chain perpendicular to the slab surface is shown. In the present case, the same profile is obtained for all the chains in the slab. It is clear, from this profile, that the two unit cells nearest to the surface develop a small polarization. This local polarization of the surface cells, at both sides of the slab, are pointing inwards towards the bulk, so the net polarization vanishes. This inward direction of the local surface polarization is just a consequence of the surface atomic relaxation pattern analyzed in the above section. Indeed, this polarization profile and the magnitude of the local polarization of the surface cells shown in Fig. 4 at $T=0$ K, remain unchanged at higher temperatures, even in the paraelectric phase.

The fact the inner cells of the slab are not polarized could arise from a surface tension effect, i.e., as a consequence of the inwards movement of the surface layers, the interior of the slab could be denser than the bulk material inhibiting ferroelectricity. To address this point, we have measured the interlayer distance between two consecutive TiO_2 planes at the surface and in the interior of the slab. While this distance is 3.89 Å at the surface, indicating that the surface layers contract substantially, it reaches the value of 3.99 Å at only two unit cells from the surface. So, the interior of the slab is not considerably denser than the bulk material. Therefore, as was already shown from the static calculations, the competition between the energy gain on the surface relaxation and the energy gain on the ferroelectric distortion seems to be crucial for the out-of-plane ferroelectricity in ultrathin films. As it is well known, ferroelectricity is strongly affected by volume in ABO_3 perovskites. In particular, the elongation of a perovskite crystal along its polar direction favors ferroelectricity in that direction. So, it would be interesting to investigate how the microscopic features obtained for the stress-free slab are affected by the lattice strain.

C. Strain effect

An important factor which can influence the ferroelectric properties of a thin film is the effect produced by the lattice mismatch between a given substrate and the film.[5] In a recent experimental work, it was demostrated that there is a considerable increase in the spontaneous polarization and out-of-plane lattice parameter in epitaxially grown thin films in comparison with relatively thicker films.[16] Both observations have been interpreted as an effect of internal stresses due to lattice mismatch. Experimental data on $BaTiO_3$ films deposited on $SrTiO_3$ substrates[17] showed a shift of T_c towards higher temperatures. They conclude that this effect should be due to epitaxial strain, showing that the lattice parameter *a* of a 10 monolayer-thick film is exactly the same as that of the substrate. So, if the substrate is sufficiently thick, the in-plane strains of the film at the interface are totally controlled by the thick substrate, which produces a two dimensional clamping and straining of the film.

In this section we investigate the strain effects on the FE properties of the slab. We assume that the above mentioned internal elastic fields are homogeneous, so the 2D clamping holds throughout the ultrathin film. So, we force the simulation cell to be square in the *x*-*y* plane with different lattice parameters. However, the simulation cell is allowed to expand and contract in the *z* direction until the *zz* component of stress is zero throughout. For the sake of simplicity, we define a misfit strain as $\eta=(b-a)/b$, where *b* is the imposed lattice constant in the *x*-*y* plane (which could be related with lattice constant of a hypothetic substrate) and *a* is the lattice parameter of the stress-free film. Since positive values of η will tend to suppress even more the out-of-plane ferroelectricity, we only investigate the effects produced by negative strains, which will tend to elongate the out-of-plane lattice constant of the slab, reinforcing ferroelectricity in that direction.

We show in Fig. 4 the $p_z(z)$ (top panel) and $p_x(z)$ (bottom panel) profiles at $T=0$ K of a randomly chosen chain perpendicular to the slab surface for different misfit strains. It is clear from this figure that, under negative strains, individual chains develop a net out-of-plane polarization. This feature seems to be in contradiction with the fact that we are simulating a not short-circuited slab, and a *monodomain*

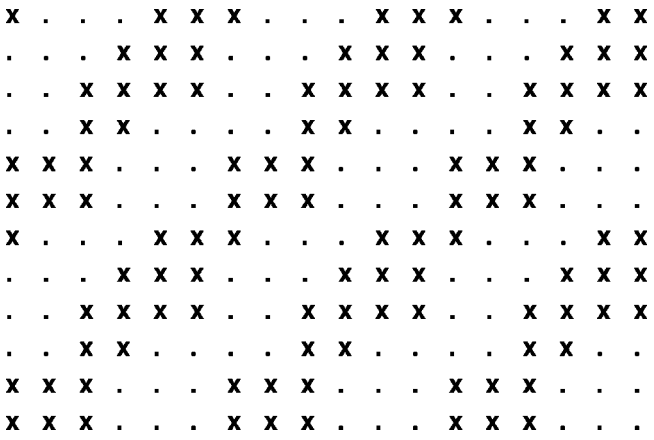

FIG. 5. Top view of the out-of-plane polarization pattern for the case $\eta=-2.5\%$. The symbols $\times$ or $\bigcirc$ on each chain denote opposite polarization directions.

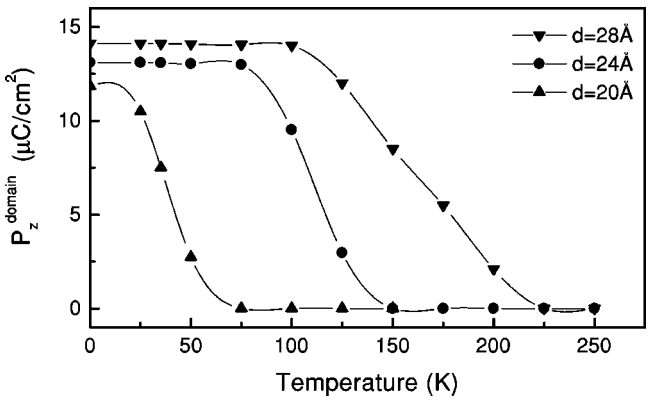

FIG. 6. Out-of-plane component (z) of the domain polarization as a function of temperature for different slab widths.

ferroelectric state should not be stabilized due to the presence of a very strong depolarizing field. However, although the individual chains shown in Fig. 4 diplay a perpendicular nonvanishing polarization, the *net* out-of-plane polarization of the slab is zero due to the development of polarized domains, as it is shown in Fig. 5 for the case $\eta=-2.5\%$. For this value of η the local polarization vector of the inner cells lies along the z direction ($p_x=p_y=0$, see Fig. 4), so 180° polarized domains are developed. However, for higher values of η ($\eta=-1.0\%$), the net in-plane polarization is not zero and the domain configuration is more complex. We can describe the behavior of the local polarization vector under strain in the following way. The stress-free film is polarized along the (110) direction. When the film is negatively strained, the polarization vector starts rotating towards the z axes. In this case a domain configuration is developed because the polarization vector rotates towards the positive z axis in one domain, while in the other it rotates in the opposite direction. Finally, at a given value of η the polarization vector of each domain lies along the z axis, giving arise to 180° polarized domains. In all cases the net out-of-plane polarization is zero and the domain wall is not charged. So, we demonstrate that a strain induced ferroelectric polydomain state with an out-of-plane orientation of the polarization is indeed stable in the ultrathin film. It is known that domains are favored because of the reduction of the depolarizing field energy in spite of the increased surface energy of the domain walls. So, if electrodes are deposited on the film surfaces cancelling out the depolarizing field, a single-domain structure is expected to become more stable. To address that point, a different boundary condition should be used, and this investigation is in progress.

It is interesting to point out that the cell-by-cell out-of-plane polarization profiles shown in the top panel of Fig. 4 display a considerable reduction of the polarization at the surface cells, indicating that the surface produces a weakening of ferroelectricity, in agreement with a phenomenological study.[3]

It is clear from Fig. 5 that the 180° domain configuration is of stripe type. It is important to remark, however, that the equilibrium value of the domain width cannot be determined from the present simulations, since this magnitude is constrained by the dimension of the simulation cell. We performed simulations using longer supercells along the x and y directions 8×8 and 10×10. In both cases we obtain similar results to the one previously reported; namely, the development of a stripe-type domain structure with a domain width of half of the supercell dimension. So, although the equilibrium value of the domain width cannot be determined in the thermodynamic limit due to computational limitations, this test constitutes a clear evidence of the existence of a ferroelectric polydomain state. We are also able to provide another valuable microscopic information: the 180° domain wall is centered on a Ba-O plane, i.e., the atomic displacements have odd symmetry across (and vanish on) the BaO plane, which indicates that the domain boundary is indeed very sharp, its width being of approximately one lattice constant, in agreement with domain walls simulations in bulk.[18]

Finally, we performed molecular dynamics simulations to determine the temperature where the out-of-plane polarization of each domain vanishes. This transition temperature is determined by monitoring the polarization of each domain as a function of temperature under heating. For the simulations we chose the case $\eta=-1.5\%$. Note that for this value of strain the in-plane polarizations of the slab are zero (see Fig. 4), so there is only one phase transition at finite temperature involving the z component of the domain polarization (P_z^{domain}). The results are shown in Fig. 6. The transition temperature obtained for the film of 28 Å width is ≈225 K. It is interesting to remark that the behavior of P_z^{domain} with temperature resembles the temperature dependence of the order parameter in a ''second-order phase transition.'' To find out which is the minimum film thickness (d_c) with stable out-of-plane ferroelectricity we have done simulations on slabs of different widths using the same mechanical boundary condition ($\eta=-1.5\%$). The results are also shown in Fig. 6. It is clear that the transition temperature decreases when the film thickness decreases. We can predict from these simulations that $d_c\approx20$ Å. It is interesting to remark that the predicted minimum film thickness is just one unit cell longer

than the minimum displacement correlation length required to observe a ferroelectric instability in bulk [$\approx$4 unit cells for $BaTiO_3$ (Ref. 19)], which would be an indication that both magnitudes could be related.

IV. CONCLUSIONS

In conclusion, we have shown, using an atomistic model for $BaTiO_3$, that (i) ferroelectric phase transitions involving in-plane electric polarization are unperturbed by the presence of the surface in ultrathin films; (ii) the effect produced by the surface is just to increase (or decrease, depending on the surface termination) the in-plane polarization of the two unit cells nearest to the surface, in such a way that the surface of the film orders at a temperature above (or below) that of the interior ordering; (iii) the competition between the energy gain on the surface relaxation and the energy gain on the ferroelectric distortion seems to be crucial for the development of a FE phase with out-of-plane polarization in an ultrathin film; but (iv) a strain induced polydomain ferroelectric state with an out-of-plane orientation of polarization can be stabilized, in a not short-circuited TiO_2-terminated film as thin as 20 Å. $P_z^{\mathrm{domain}}(z)$, which is a key information for Landau-Devonshire type theories, diplays a weakening of the polarization at the surface. Finally, we point out that the development of polarized domains in the film constitutes a promising starting point for a further investigation on the microscopic mechanism for the poling and polarization switching processes when an external electric field is applied.

We acknowledge R. Migoni, M. Sepliarsky, and S. Phillpot for stimulating discussions. This work was supported by CONICET-Argentina. M.G.S. thanks Aspen Center for Physics and the support of CIUNR and FONCyT.

[1] J. F. Scott, *Ferroelectric Memories*, Vol. 3 of Springer Series in Advanced Microelectronic (Springer-Verlag, Berlin, 2000).
[2] T. Tybell, C. Ahn, and J. M. Trisone, Appl. Phys. Lett. **75**, 856 (1999).
[3] Y. G. Wang, W. L. Zhong, and P. L. Zhang, Phys. Rev. B **51**, 5311 (1995).
[4] A. M. Bratkovsky and A. P. Levanyuk, Phys. Rev. Lett. **84**, 3177 (2000).
[5] N. A. Pertsev, A. G. Zembilgotov, and A. K. Tagantsev, Phys. Rev. Lett. **80**, 1988 (1998).
[6] N. A. Pertsev, A. K. Tagantsev, and N. Setter, Phys. Rev. B **61**, R825 (2000).
[7] R. E. Cohen, J. Phys. Chem. Solids **57**, 1393 (1996); Ferroelectrics **194**, 323 (1997).
[8] J. Padilla and D. Vanderbilt, Phys. Rev. B **56**, 1625 (1997); M. Meyer, J. Padilla, and D. Vanderbilt, Faraday Discuss. **114**, 395 (1999).
[9] Ph. Ghosez and K. M. Rabe, Appl. Phys. Lett. **76**, 2767 (2000).
[10] S. Tinte, M. G. Stachiotti, M. Sepliarsky, R. L. Migoni, and C. O. Rodriguez, J. Phys.: Condens. Matter **11**, 9679 (1999).
[11] W. Zhong, D. Vanderbilt, and K. Rabe, Phys. Rev. Lett. **73**, 1861 (1994).
[12] S. Tinte, M. G. Stachiotti, M. Sepliarsky, R. L. Migoni, and C. O. Rodriguez, Ferroelectrics **237**, 41 (2000).
[13] DL-POLY is a package of molecular simulation routines written by W. Smith and T. R. Forester, Daresbury and Rutherford Appleton Laboratory, Daresbury, UK.
[14] S. Tinte and M. G. Stachiotti, in *Fundamental Physics of Ferroelectrics*, edited by Ronald Cohen, AIP Conf. Proc. No. 535 (AIP, Melville, 2000), p. 273.
[15] R. A. McKee, F. J. Walker, E. D. Specht, G. E. Jellison, Jr., L. A. Boatner, and J. H. Harding, Phys. Rev. Lett. **72**, 2741 (1994).
[16] V. Nagarajan, I. G. Jenkins, S. P. Alpay, H. Li, S. Aggarwal, L. Salamanca-Riba, A. L. Roytburd, and R. Ramesh, J. Appl. Phys. **86**, 595 (1999).
[17] Y. Yoneda, T. Okabe, K. Sakaue, H. Terauchi, H. Kasatani, and K. Deguchi, J. Appl. Phys. **83**, 2458 (1998).
[18] J. Padilla, W. Zhong, and D. Vanderbilt, Phys. Rev. B **53**, R5969 (1996).
[19] P. H. Ghosez, X. Gonze, and J.-P. Michenaud, Ferroelectrics **206**, 205 (1998).